Model-based design of closed loop controllers of the air-path in a heavy duty diesel engine

Model-based design of closed loop controllers of the air-path in a heavy duty diesel engine

Cite as: AIP Conference Proceedings **2191**, 020152 (2019); https://doi.org/10.1063/1.5138885
Published Online: 17 December 2019

Loris Ventura, Roberto Finesso, Stefano A. Malan, Stefano d'Ambrosio, and Andrea Manelli

Model-based Design of Closed Loop Controllers of the Air-path in a Heavy Duty Diesel Engine

Loris Ventura[1,a)], Roberto Finesso[1], Stefano A. Malan[2], Stefano d'Ambrosio[1] and Andrea Manelli[1]

[1]*Politecnico di Torino, Department of Energy, C.so Duca degli Abruzzi 24, 10129, Torino, Italy.*
[2]*Politecnico di Torino, Department of Electronics and Telecommunications, C.so Duca degli Abruzzi 24, 10129, Torino, Italy.*

[a)]Corresponding author: loris.ventura@polito.it

Abstract. Diesel powertrains will remain an indispensable energy carrier to meet the CO_2 emission targets in the short-term for both light-duty and heavy-duty applications. As the legislation limits become more and more stringent, innovative solutions are developed in order to meet them. The recent advances in the performance of Electronic Control Units (ECUs) and sensors made it possible to use model-based control strategies rather than the classical map-based approach. In this paper, two different closed loop controllers of the air-path of a heavy-duty diesel engine have been designed and compared through the Model-in-the-Loop (MiL) technique by using the GT-Power software as engine simulator. The design of the controllers was carried out by using a model-based approach. In particular, a detailed model of the engine, realized using the GT-Power 1D commercial code, was simplified and linearized at 5 selected engine points using the ARX black-box identification approach. These linearized models were then used to tune the developed controllers. The whole design has the goal of ensuring the correct engine functioning while affecting the formation of NO_x emissions. The behavior of two control structures, PID and Eigenvalue placement, has been compared. The actuated variables are the positions of EGR and VGT actuators while the controlled ones are the oxygen concentration in the intake manifold and the boost pressure. The choice of the intake oxygen concentration as control variable is directly connected to its strict correlation with the pollutant emissions (in particular, with NO_x emissions), in order to control them in a more effective way, especially in transient operation.

INTRODUCTION

Emission limit legislations have become more and more severe in the last decade as the attention and concern on environment and climate changes has grown. The automotive industry introduced a wide range of technological solutions to meet these standards. Exhaust Gas Recirculation (EGR) and Variable Geometry Turbochargers (VGTs) [1], high pressure common rail injection systems [2–6], advanced combustion control and innovative combustion concepts [7, 8] represent some of these technologies. Among these technologies, the development of advanced controllers is becoming more and more important, also due to the possibility of integration with the emerging V2V and V2I systems.

Regarding the heavy-duty vehicles, it is generally agreed that diesel engines will remain the main propulsion system at least for the following 20-30 years. Therefore the research effort in this field is moving towards the development of control strategies that take directly into account the pollutants. This work investigates the performance of a closed loop air-path controller designed to control the boost pressure and the intake oxygen concentration, by acting on the VGT and EGR valve positions. The choice of controlling the intake O_2 concentration instead, for example, of the intake air mass (as is usually done in conventional controllers) is due to its strict correlation with the pollutant emissions (in particular NO_x, as will be shown in the 'PROBLEM DEFINITION' section).

Conventional controllers are usually based on maps (feed-forward controllers) or PIDs (closed-loop controllers) [9]. Although very common, they however may lack of efficacy especially concerning the control of emissions in transient operation. Therefore, interest in the development of innovative controllers (especially of the model-based type) is increasing. Several examples of model-based controllers have been reported in the literature, such as predictive control [10] and H_∞ [11], but control strategies as neural network and fuzzy control [12] are also of interest despite

74th ATI National Congress
AIP Conf. Proc. 2191, 020152-1–020152-9; https://doi.org/10.1063/1.5138885
Published by AIP Publishing. 978-0-7354-1938-4/$30.00

their complexity and counter-intuitive tuning of their parameters. In addition to the nature of the controller, also the selection of the most suitable control variables plays a crucial role. Intake Manifold Pressure (IMAP) and fresh Air Mass Flow (MAF) have been extensively used due to the presence of dedicated sensors installed on engines. However the fresh air mass flow is not strictly connected to pollutants, consequently emission control through its use is not easy and effective. Other variables with a closer connection with pollutants are EGR flow and fraction, Lambda (i.e., relative air-to-fuel ratio) and intake oxygen concentration [13]. In the present paper, the intake manifold pressure and the intake oxygen concentration have been selected as control variables.

Nomenclature

ARX	Auto Regressive eXogenous
BMEP	Brake Mean Effective Pressure
EIGP	EIGenvalue Placement
EGR	Exhaust Gas Recirculation
IMAP	Intake Manifold Pressure
MAF	fresh Air Mass Flow
MiL	Model-in-the-Loop
MIMO	Multiple-Input Multiple-Output
RAF	Relative Air Fuel Ratio
RPM	Engine Speed
VGT	Variable Geometry Turbochargers
V2I	Vehicle-to-Infrastructure
V2V	Vehicle-to-Vehicle

PROBLEM DEFINITION

The considered diesel engine is a FPT cursor 11. It is an 11-liter, 6-cylinder engine provided with high pressure EGR and VGT.

The choice of the variables to use in the control system is the first fundamental step to undertake. Looking at the air-path layout of the cursor 11 engine, the two available actuators are the EGR and VGT valves. Consequently they have been used as manipulated variables '$u(t)$'. In order to choose the controlled variables '$y(t)$' the correlation between different engine variables and pollutant emissions (in particular, NO_x) has been investigated. Experimental tests, including an intake oxygen sweep, were performed on the real engine. Measurements were made in different points over the whole engine map that are indicated with the blue '+' signs in Fig. 1. The meaning of the other signs will be explained in the next sections. In order to select the best control variables of the air path controller, a correlation analysis has been carried out considering NO_x emissions, which are one of the major pollutants for diesel engines.

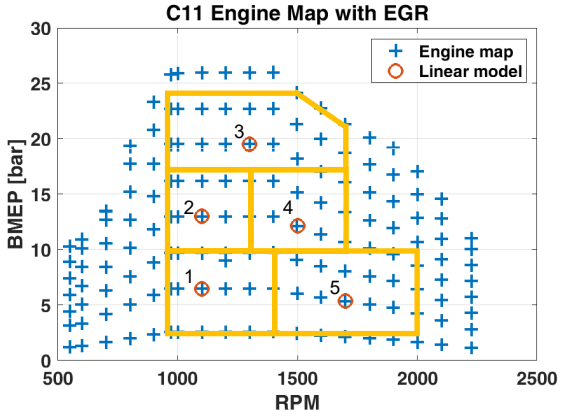

FIGURE 1. Cursor 11 engine map.

First, the control variables typically used in conventional controllers, i.e., MAF and IMAP, have been considered. The correlation between MAF and NO_x emissions is shown in Fig. 2a. The graph shows that the MAF-NO_x correlation is influenced more by the load than by the engine speed and as the load grows more NO_x are emitted. Also low speed points do not show a defined behavior as they are distributed over a wide area. As the load increases the points shift to the right side, toward higher MAF values, and a trend can be identified. However this trend is nonlinear and the impossibility to find a good correlation at low loads makes the MAF a poor indicator of the NO_x emissions. In the case of IMAP (Fig. 2b) no correlation or trend can be identified at low speed. It is only possible to define a zone in which low load points are concentrated. Also in this case as the load increases the situation improves but the correlation that can be identified is again nonlinear. Such situation suggests that the IMAP variable does not provide a valuable insight for the NO_x control, while it is generally correlated to the indicated torque and to the soot emissions.

Variables with a known influence on pollutant formation are EGR mass flow and fraction, Lambda and intake oxygen concentration. NO_x formation is strictly related to the temperature reached in the combustion process. Through the recirculation of exhaust gases the combustion peak temperature is lowered. By plotting the EGR mass flow rate vs. the NO_x emissions (Fig. 2c), it can be seen that two distinct trends exist. The first one includes lower load points (which are associated to lower NO_x emissions) while the second one includes higher load points (which are associated to higher NO_x emissions). At fixed engine point, the NO_x production decreases as the EGR mass flow rate increases. The relation is however nonlinear as, for every engine point, the last part of the curve corresponding to high EGR rates forms a bend toward the horizontal axis. Furthermore the EGR mass flow rate cannot be directly measured but has to be estimated. For these last two reasons the EGR mass flow rate has been discarded. However details on the effect of EGR can be found in [14]. Considering the Relative Air Fuel Ratio (RAF), Fig. 2d shows that the distribution of the points assumes the shape of a funnel. High load points correspond to low RAF values and high NO_x emissions while low load points are associated with high RAF values and low NO_x emissions. For these points the correlation is nonlinear but can be approximated by a second order curve. At low load the situation worsen as the points become scattered. Thus it is not easy to find an effective correlation for these conditions. Rather than on NO_x, it was found experimentally that the RAF has a strong influence on Particulate Matter. A detailed explanation can be found in [15]. Figure 2e shows the O_2-NO_x correlation. It can be seen that the correlation is basically linear. The slope of the straight line increases as the load increases and decreases as the speed increases. From Fig. 2e it can also be noted that NO_x increases as O_2 increases. From the above comments it is now clear why O_2 has been chosen as a control variable of the air path controller. It in fact has a linear relation with NO_x emissions over the whole engine map and is influenced in a definite manner by load and speed. As a consequence, an accurate control of the intake O_2 concentration can lead to an accurate control of NO_x emissions. To complete the variable selection, dealing with the engine performance, the intake manifold pressure has been chosen as controlled variable as is usually done in conventional air path controllers.

MODELING OF THE ENGINE RESPONSE

The second step toward the design of the control system is to set-up a model to be used for the design and tuning of the controllers. Various approaches exist in the literature, but those which are adopted more frequently are the physical and the black box modeling. The first one is based on the physical modeling of the system using basic equations such as the conservation of mass and energy. The second one is constituted by mathematical models which are derived from observed data. In this work the black box approach has been used, but an example of physical model can be found in [16]. The details of the identification procedure can be found in [17].

The identification tests were carried out on an engine simulation software, i.e., GT-Power. The GT-Power model has been calibrated on experimental measurements taken over the real engine. Starting from the GT-power model of the engine, simplified linear models were then derived at selected engine points, in order to design and tune the controllers. In this work 5 linear models were estimated; one for each point as shown in Fig. 1 with red circles. The selected model structure is the Auto Regressive eXogenous (ARX). Input-output models of this family are described by linear difference equations such as Eq. 1

$$y(t) + a_1\, y(t-1) + ... + a_{n_a}\, y(t-na) = b_1\, u(t-n_k) + ... + b_{n_b}\, u(t-n_b-n_k+1) + w(t) \tag{1}$$

where na, nb and nk define the orders of the model. The $w(t)$ term represents the stochastic noise that affects this process. In the following the ARX model structure will be denoted with ARX [na nb nk]. The coefficients na and nb determine how far the time history of the system affects the actual output, while nk defines the dead time, i.e., the number of samples that have to pass before the input affects the output. For a complete explanation see [18]. Preliminary

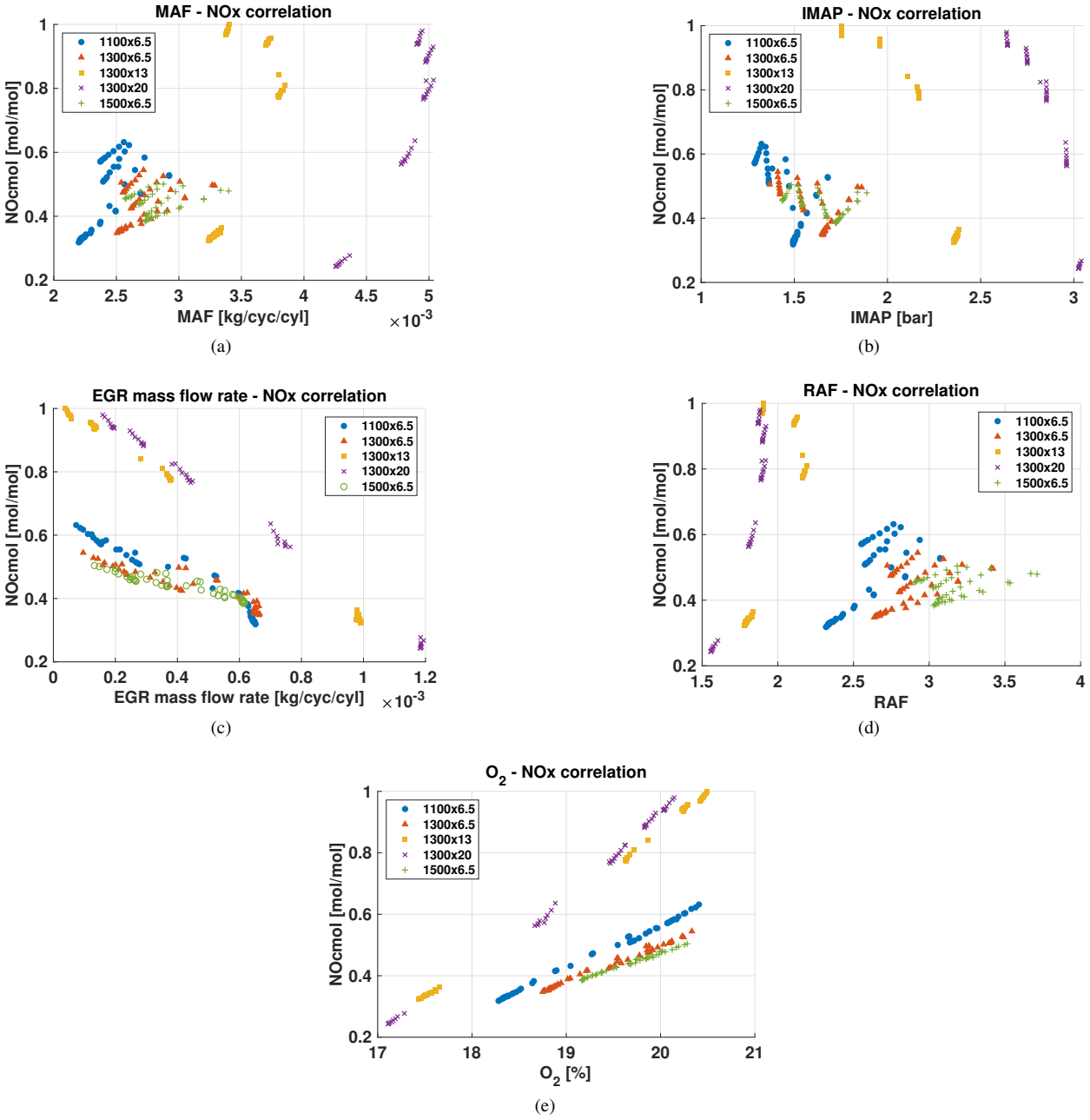

FIGURE 2. Engine variables correlation with NO_x. a) MAF-NO_x; b) IMAP-NO_x; c) EGRmass flow rate-NO_x; d) RAF-NO_x; e) O_2-NO_x

tests among different orders were conducted to establish it. From these tests, the ARX [2 1 0] structure was chosen. As the models use the EGR and VGT valve position as input variables, and they return the intake O_2 concentration and the IMAP as output variables, they are defined as Multiple-Input Multiple-Output (MIMO). In this considered case the inputs and the outputs are two. Equations 2 and 3 show the structure of a two-input two-output ARX [2 1 0] model.

$$y_1(t) + a_{1,1,1}\, y_1(t-1) + a_{1,1,2}\, y_1(t-2) + a_{1,2,1}\, y_2(t-1) + a_{1,2,2}\, y_2(t-2) = b_{0,1}\, u_1(t) + b_{0,2}\, u_2(t-1) + w(t) \quad (2)$$

$$y_2(t) + a_{2,2,1}\, y_2(t-1) + a_{2,2,2}\, y_2(t-2) + a_{2,1,1}\, y_1(t-1) + a_{2,1,2}\, y_1(t-2) = b_{0,2}\, u_2(t) + b_{0,1}\, u_1(t-1) + w(t) \quad (3)$$

The difference between Eq. 1 and 2 (or 3) are the terms representing the mutual influence between inputs and outputs. For the identification process the system was perturbed actuating the EGR and VGT valves through square waves.

Since this was a preliminary study on the development of a control system which is based on O_2-IMAP variables, the entire engine map has not been investigated. The work only focused on the area in which experimental information on the intake oxygen concentration was available. Based on this, 5 engine points have been selected as shown in Fig.1 (red circles) and they represent the engine behaviour in the corresponding rectangular area (in yellow). Regions of the engine map close to its boundary (full load, low speed-high/low load and high speed-high/low load) have been excluded. However, by estimating additional linear models in other engine functioning points the whole engine map can be covered.

Considering that linearized models work around a single engine point, the variation of the inputs and outputs was considered in both the identification and validation processes. Furthermore, in the identification procedure scaling and de-trending the signals reduces systematic and numerical errors.

In Fig. 3 the validation results of the ARX [2 1 0] model for the engine point 1, i.e., 1100RPM x 6.5bar, are shown. Figure 3a shows the O_2 trend predicted by the identified linear model (red lines) over the O_2 trend predicted by the GT-power model (black dashed line). Apart some differences in the peaks, the linear model well reproduces the dynamics of the O_2 showing a fitting of 81%. Figure 3b shows the IMAP validation. The predicted values from the ARX model are reported with red lines while the GT-Power values in black dashed line. Here the identified model captured all the dynamics of the system showing a fitting of 97%.

Equation 4 and Eq. 5 represent the ARX [2 1 0] model above mentioned for the engine point 1, 1100RPM x 6.5bar. The model for predicting the O_2 is given in Eq. 4 while Eq. 5 represents the model for the IMAP. Looking at Eq. 4 and 5 it can be noted that every input is linked with every output through different polynomials. These links can be referred as channels and in this case 4 channels can be defined: 1) EGR to O_2; 2) EGR to IMAP; 3) VGT to O_2; 4) VGT to IMAP.

$$y_{O_2}(t) - 0.5820\, y_{O_2}(t-1) - 0.0017\, y_{O_2}(t-2) - 1.8499\, y_{IMAP}(t-1) + 1.1637\, y_{IMAP}(t-2) = 0.0257\, u_{EGR} + 0.8555\, u_{VGT} + w(t) \tag{4}$$

$$y_{IMAP}(t) - 1.4646\, y_{IMAP}(t-1) + 0.05647\, y_{IMAP}(t-2) - 0.0144\, y_{O_2}(t-1) + 0.0057\, y_{O_2}(t-2) = -0.0805\, u_{VGT} + 8.5104e{-}5\, u_{EGR} + w(t) \tag{5}$$

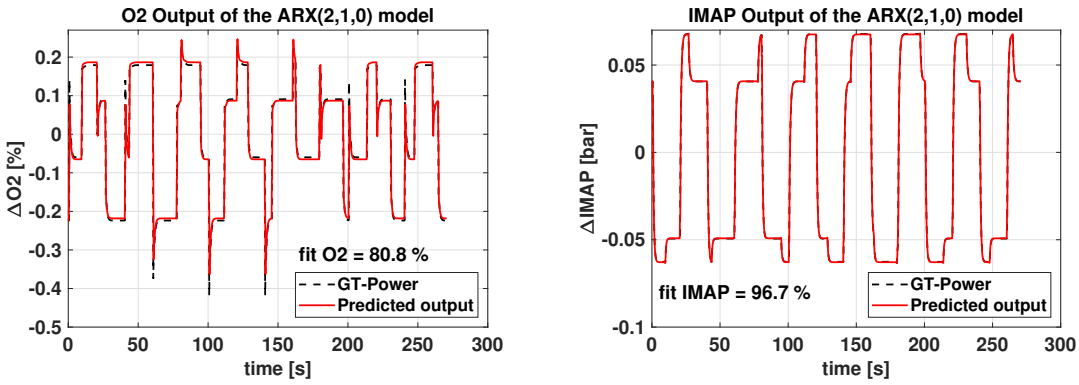

(a) (b)

FIGURE 3. Engine point 1, i.e. 110RPM x 6.5bar, ARX [2 1 0] validation. a) O2 channel; b) IMAP channel.

CONTROL DESIGN

The design process of the controller has been carried out for each of the 5 engine map points. For every considered engine point two control strategies were compared. These are the PID and EIGenvalue Placement (EIGP) control.

The PID is a well know control techniques whose control law is expressed by Eq.6.

$$u(t) = K_p e(t) + K_i \int_0^t e(\tau)d\tau + K_d \frac{de(t)}{dt} \tag{6}$$

The scheme of the PID controller is indicated in Fig. 4a. Its design in this work has been carried out considering the system as decoupled. In particular, the EGR valve position was used to target the intake O_2 concentration while the VGT position was used to target the boost pressure. Following this approach, the two PID compensators, work independently seeing each other correction as a disturbance. In Fig. 4a the error $e(t)$ is also shown.

The EIGP is a linear control techniques which is realized through the adoption of static linear control action of the form of Eq. 7.

$$u(t) = -\mathbf{K}x(t) \tag{7}$$

Through the gain vector **K** it is possible to impose the desired dynamics that is associated to the system eigenvalues. In Eq. 7 $x(t)$ represents the system states. The knowledge of the latter variables, together with the knowledge of the input variables, allows to completely determine the behavior of a dynamic system. The states can be defined from physical variables or they can be purely mathematical. For this reason, the states are not restrained to physical systems, but they can be defined for any type of system. In order to have zero error at steady state condition, an integrator has been added in the control loop. The architecture is shown in Fig. 4b. For further details about the two control structures see [19]. Due to its properties, differently from the PID, the EIGP is able to deal with the coupled system resulting thus in a MIMO control. The EIGP tuning procedure was performed according to the principle of

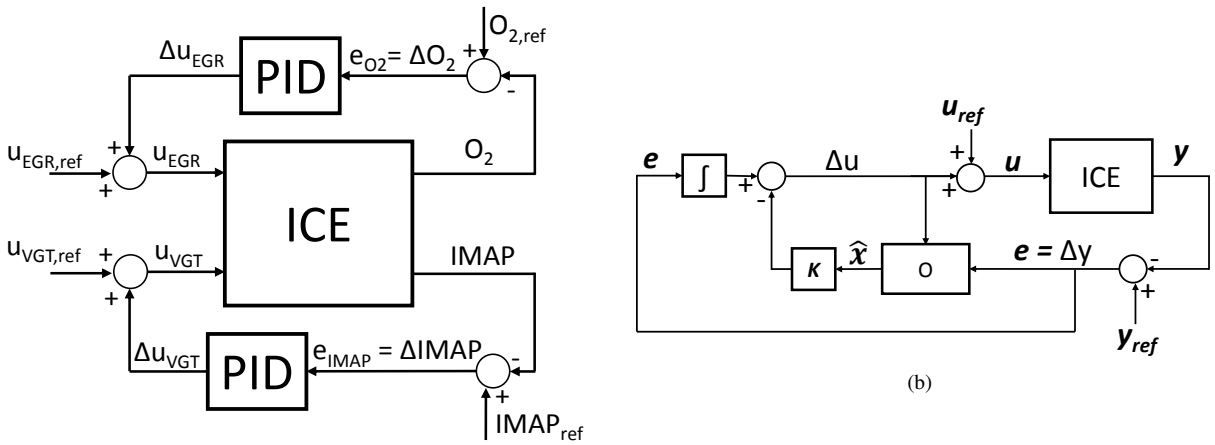

FIGURE 4. Control schemes: a) PID; b) EIGP

2nd order dominant poles. It consists in choosing the damping and natural frequency such that the controlled system shows the desired behavior. An observer was also introduced in order to retrieve the system states. This was needed since the identified model is a purely mathematical object and its states have no direct physical meaning.

RESULTS

The designed control systems were tested by means of the co-simulation between Simulink and GT-Power (Model-in-the-Loop technique).

Figure 5 shows the results for engine point 1 corresponding to a low load/low speed condition. Considering the O_2 (Fig. 5a) both controllers show an acceptable behavior. It can be seen in the figure that at t=20s a step of intake O2 request (from 20.83 to 20.96%) occurs. Both the control systems are able to drive the O_2 close to the reference value. The two control systems have a similar response, even though the PID one shows a larger overshoot and a faster settling time than the EIGP. At time t=35s the IMAP reference step is applied (Fig. 5b) and both the control systems

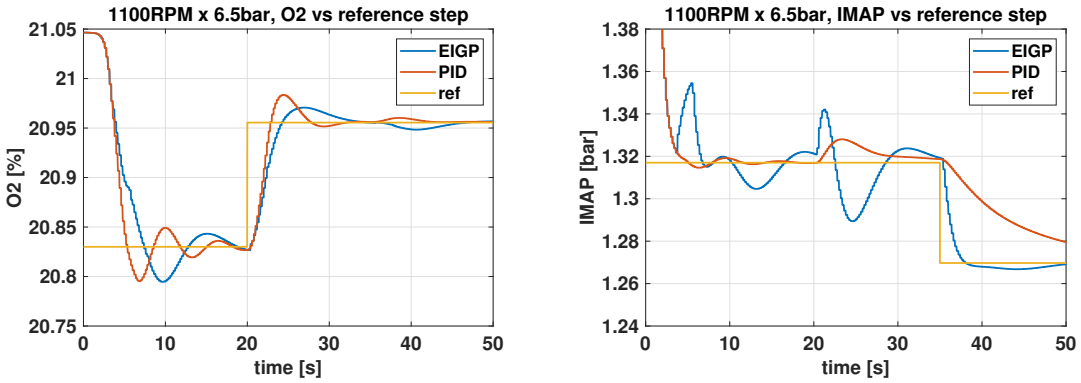

(a) (b)

FIGURE 5. Comparison of EIGP vs PID performance over the two outputs. Engine point 1: 1100RPM x 6.5bar. a) O_2 b) IMAP.

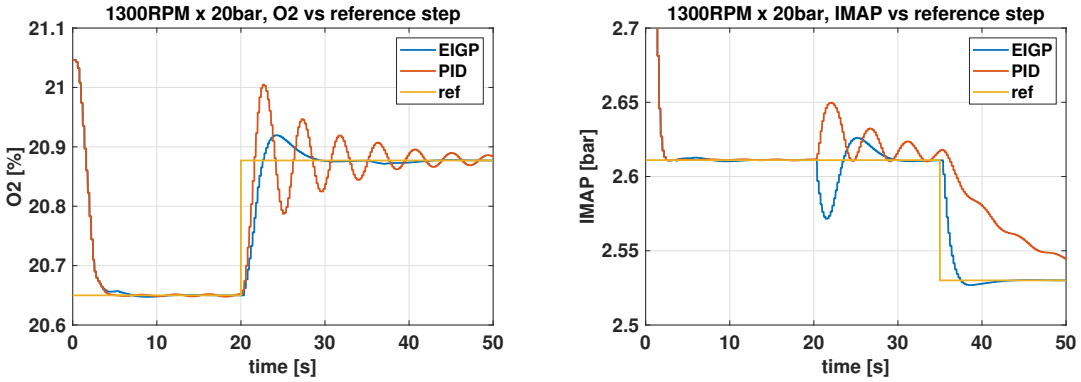

(a) (b)

FIGURE 6. Comparison of EIGP vs PID performance over the two outputs. Engine point 3: 1300RPM x 20bar. a) O_2; b) IMAP.

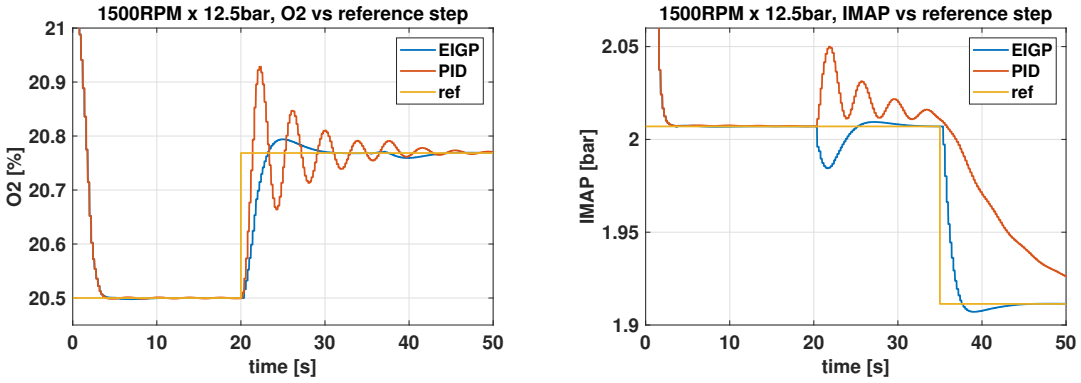

(a) (b)

FIGURE 7. Comparison of EIGP vs PID performance over the two outputs. Engine point 4: 1500RPM x 12.5bar. a) O_2; b) IMAP.

are able to maintain the O_2 reference. Instead by looking at the IMAP trends in Fig. 5b a clear difference between the two control system behavior is visible. During the initial startup transient the EIGP controller shows an oscillatory

behavior while the PID does not. When the O_2 step is applied (time t=20s) the EIGP control action has a larger impact on the IMAP that the PID, but when the IMAP step is applied (time t=35s) the EIGP controller is able to follow the reference while the PID is not.

In Fig. 6 a high load condition corresponding to the engine point 3 is shown. The results reported in Fig. 6a indicate that, concerning the O_2 control, the PID shows an undesired behaviour, since the output oscillates and the convergence is not reached in satisfactory time. On the other hand the EIGP is able to follow the reference in a smooth way and to compensate the disturbance of the IMAP step at time t=35s. Regarding the startup transient both the control systems are able to drive the system at the nominal condition of the considered engine point. Concerning the control of IMAP (Fig. 6b), it can be noted that the PID is not able to get back from the O_2 step and to follow the IMAP step either. The EIGP instead shows a good response to the IMAP step occurring at time t=35s. At time t=20s the effect of the O_2 step on this channel is visible.

The results for engine point 4 corresponding to 1500RPM x 12.5bar are shown in Fig. 7. In Fig. 7a it is visible that only the EIGP is able to follow the O_2 step at time t=20s. The PID shows an undesired damped oscillating behavior. At time t=35s the effect of the IMAP step over the O_2 is visible. The IMAP results are shown in Fig. 7b: also in this engine point the PID is not effective in controlling the IMAP. On the other hand the EIGP well compensates the O_2 step influence and is able to follow the IMAP step at time t=35s.

The above mentioned results highlight the advantage related to the MIMO property of the EIGP, as it is able to consider the whole system together exploiting the mutual influence between the channels. On the contrary the PID performance is limited by the decoupling procedure needed for this type of controller. The action of a channel is seen as a disturbance from the other one. This imposes a limit in terms of readiness (transient response) on one of the two controllers, otherwise the situation depicted in Fig. 6 and 7 occurs. This problem is also due to the nature of the chosen controlled variables (O_2 and IMAP). The O_2 is influenced by both EGR and VGT and can be referred as a 'global' variable. The IMAP instead mainly depends on the VGT with a small influence of the EGR valve. In other words, in order to regulate the O_2 the joint operation of EGR and VGT is required, while to control the IMAP only the VGT actuator can be used. In the PID design process the one controlling the O_2 was set to be faster than the IMAP one. For this reason the PID resulted to be unable to follow the IMAP reference in Figs. 5b, 6b and 7b. With reference of the O2 control, by comparing the behaviour of the PID and EIGP for the three considered engine points (Figs. 5a, 6a, 7a), it can be noted that as the load increases the EIGP behavior improves becoming smoother. This happens also for the IMAP control, as can be seen in Figs. 5b, 6b and 7b. Furthermore, with reference to the IMAP control, as the load increases the influence of the O_2 grows and the EIGP control system thanks to its MIMO characteristic is able to manage the phenomena occurring in the air path also when they intensify. On the contrary the PID performance worsen as the engine load increases for both the control variables, O_2 and IMAP. For the sake of brevity the results for the other two engine points are omitted but they are in accordance with what has been written above.

As a further and more severe test at every engine point, both the control systems were tested against a square wave and also this case has demonstrated the advantages of the EIGP over the PID.

CONCLUSIONS

In this paper, two different strategies, namely PID and EIGP, have been developed for the air path control of a heavy-duty diesel engine. The performance of the two controllers has been compared over various operating points of the engine map by means of the Model-in-the-Loop (MiL) technique. Both control systems use the positions of EGR and VGT actuators as manipulated variables and oxygen concentration in the intake manifold and boost pressure as controlled variables. The development of the control system has been carried out in MATLAB/Simulink environment while GT-Power was used as engine emulator for the identification and control evaluation test. Steps and square wave signals have been used to test the two control systems. Comparing the two controllers, the EIGP has proven to be more effective than the PID controller in all the tested points, since it was able to deal with the whole coupled system ensuring a suitable behavior for the application. The PID suffered the mutual influence of the channels thus resulting not able to manage the two outputs together. Future activities will focus on the adjustment of the control system for calibration purposes through Hardware in the Loop (HiL) and Rapid prototyping.

REFERENCES

[1] M. Baratta, R. Finesso, D. Misul, and E. Spessa, Comparison between internal and external egr performance on a heavy duty diesel engine by means of a refined 1d fluid-dynamic engine model, sep 2015.

[2] A. Ferrari, A. Mittica, P. Pizzo, and Z. Jin, International Journal of Automotive Technology **19**, 771–781Oct (2018).

[3] A. Ferrari, A. Mittica, P. Pizzo, X. Wu, and H. Zhou, Journal of Engineering for Gas Turbines and Power **140**, p. 10Oct (2017).

[4] A. Ferrari, A. Mittica, F. Paolicelli, and P. Pizzo, Energy Procedia **101**, 878 – 885 (2016), aTI 2016 - 71st Conference of the Italian Thermal Machines Engineering Association.

[5] A. E. Catania, A. Ferrari, A. Mittica, and E. Spessa, "Common rail without accumulator: Development, theoretical-experimental analysis and performance enhancement at di-hcci level of a new generation fis," in *SAE World Congress & Exhibition* (SAE International, 2007).

[6] A. E. Catania, A. Ferrari, and A. Mittica, "High-pressure rotary pump performance in multi-jet common rail," in *Proceedings of 8th Biennial ASME Conference on Engineering Systems Design and Analysis, ESDA2006. Engineering Systems Design and Analysis*, Fatigue and Fracture, Heat Transfer, Internal Combustion Engines, Manufacturing, and Technology and Society, Vol. 4 (American Society of Mechanical Engineering, 2006), pp. 557–565.

[7] R. Finesso, G. Hardy, A. Mancarella, O. Marello, A. Mittica, and E. Spessa, Energies **12** (2019), 10.3390/en12030460.

[8] S. D'Ambrosio, F. Gaia, D. Iemmolo, A. Mancarella, N. Salamone, R. Vitolo, and G. Hardy, "Performance and emission comparison between a conventional euro vi diesel engine and an optimized pcci version and effect of egr cooler fouling on pcci combustion," in *WCX World Congress Experience* (SAE International, 2018).

[9] S. A. Malan and L. Ventura, "Air-path control for a prototype pcci diesel engine," in *2018 26th Mediterranean Conference on Control and Automation (MED)* (2018), pp. 843–848.

[10] P. Ortner and L. del Re, IEEE Transactions on Control Systems Technology **15**, 449–456May (2007).

[11] X. Wei and L. del Re, Control Systems Technology, IEEE Transactions on **15**, 406 – 41506 (2007).

[12] I. Abidi, J. Bosche, A. E. Hajjaji, and A. Aguilera-Gonzalez, "Fuzzy robust tracking control with pole placement for a turbocharged diesel engine," in *21st Mediterranean Conference on Control and Automation* (2013), pp. 1417–1422.

[13] J. Heywood, *Internal Combustion Engine Fundamentals 2E* (McGraw-Hill Education, 2018).

[14] A. F. S. d'Ambrosio and E. Spessa, JOURNAL OF ENGINEERING FOR GAS TURBINES AND POWER **135**, 081601–1–081601–13 (2013).

[15] R. Finesso, D. Misul, and E. Spessa, Energy Conversion and Management **84**, p. 374–38908 (2014).

[16] L. Eriksson and L. Nielsen, *Modeling and Control of Engines and Drivelines*, Automotive (Wiley) (Wiley, 2014).

[17] S. A. Malan and L. Ventura, "A systematic procedure for engine air-path identification," Tech. Rep. (Torino, 2019).

[18] L. Ljung, *System Identification: Theory for the User* (Pearson Education, 1998).

[19] K. Ogata, *Modern Control Engineering*, Instrumentation and controls series (Prentice Hall, 2010).